Differential Cross-Section Representation from Dispersion Relations: A Regge Pole Approach

A. Haffad, Z. Felfli, A. Z. Msezane, and D. Bessis
Department of Physics and Center for Theoretical Studies of Physical Systems, Clark Atlanta University, Atlanta, Georgia 30314
(Received 22 June 1995)

A dispersion relation for electron differential cross sections in the momentum transfer squared K^2, at *fixed energy*, leads to a complex angular momentum Regge pole representation. This description, which embeds the more reliable large scattering angular measurements, allows an accurate extrapolation of the generalized oscillator strength down to $K^2 = 0$, giving the optical oscillator strength. The Xe $P_{3/2}$ and $P_{1/2}$ data at 100 and 500 eV are used to illustrate the method. An experimental protocol is described for this procedure which results in a reduction of experimental noise and fluctuations.

PACS numbers: 34.80.Dp, 32.70.Cs

Lassettre, Skerbele, and Dillon [1] have deduced that the generalized oscillator strength (GOS) converges to the optical oscillator strength (OOS) as $K^2 \to 0$ (this is referred to as the Lassettre limit theorem). Additionally, they inferred that their result should be valid also for inelastic electron transitions, regardless of the applicability of the Born approximation, namely, at any impact energy E. The limiting behavior of the GOS as $K^2 \to 0$ is important in the normalization of the experimentally determined relative differential cross sections (DCS) for excitation of atoms by electron impact [2,3], calculation of cross sections for energy transfer [4], and in the determination of the OOS's [5,6]. The limiting behavior of the GOS as $K^2 \to 0$, has been examined [5,7,8] with no clear departure from the limit theorem. Therefore, one of the major theoretical difficulties is that, for finite E, the value $K^2 = 0$ is nonphysical, and it is necessary to use an interpolation-extrapolation algorithm on the experimental data to reach it. Also, accurate measurements of the DCS at small scattering angles are difficult to obtain and the experimental errors increase dramatically as the angle approaches zero, particularly for optically allowed transitions.

For the GOS, many authors use [9]

$$F(K^2) = \frac{1}{(1 + x^2)^6}\left[f_0 + \sum_{n=1}^{m} f_n \left(\frac{x^2}{1 + x^2}\right)^n \right], \quad (1)$$

where f_0 is the OOS and $x = K/Y$ with $Y = \sqrt{2I} + \sqrt{2(I - W)}$, I and W being the ionization and excitation energies, respectively. The exponent "6" is associated with the $s \to p$ transitions that we specifically study in this Letter. $F(K^2)$ is analytic in the cut complex K^2 plane from minus infinity to zero. A formula like Eq. (1) represents $F(K^2)$ by a rational fraction with a pole of order $m + 6$ located at $K^2 = -Y^2$. The discontinuity of the cut has been replaced by a pole of high degree $m + 6$. This kind of fitting procedure for the GOS suffers the deficiency of involving only data coming from small scattering angles where measurements have generally large systematic errors. This is even more transparent through the examination of the law of growth of the coefficients f_n which shows that Eq. (1) is inappropriate for large values of K^2. For example, the data [5] at 100 eV in the $J = 3/2$ state leads to $f_0 = 0.222$, $f_1 = -1.204$, $f_2 = -3.980$, and $f_3 = 30.49$. Clearly, each new term in Eq. (1) is a *much larger correction* than the previous one. Even at small values of K^2, this feature is a source of ill-conditioning from the start.

This Letter presents a new method which is unbiased, model independent, based on first principles, and correctly embeds the large scattering angle measurements where the errors are relatively small. It extrapolates reliably the GOS through the nonphysical region to $K^2 = 0$ independently of the fact that it will also represent the full scattering data including the *hump*. Previously, Gerjuoy and Krall [10], followed by Rubin, Sugar, and Tiktopoulos [11] and Tip [12], analyzed atomic scattering problems using the *energy* dispersion relation at fixed real scattering angles. While additional poles and branch cuts are introduced due to the composite nature of the target and electron exchange, when one deals with *energy* dispersion relations, no such singularities and associated difficulties are encountered in *momentum transfer dispersion relations* [13].

At *fixed physical energy*, one can write the GOS function as

$$F(x^2) = \int_0^\infty \frac{\rho(\xi)\, d\xi}{1 + \xi x^2}, \quad (2)$$

where x is the momentum transfer measured in Y units. Equation (2) defines a function of x^2 analytic in all the complex x^2 plane from $-\infty$ to 0. In particular, Eq. (2) defines a *unique and nonambiguous* analytic continuation of $F(x^2)$ from the physical positive range of values of x^2 down to zero. An equivalent but more suitable representation of Eq. (2) is

$$F(x^2) = \sum_j \frac{\rho_j}{(1 + \xi_j x^2)^{n_j}}. \quad (3)$$

 0031-9007/96/76(14)/2456(4)$10.00

Practically, only a finite number of terms in Eq. (3) is considered. If only one term is kept in Eq. (3), one gets

$$F(x^2) = \frac{F(0)}{(1 + \xi x^2)^n}, \tag{4}$$

which, when $n = 6$ and $\xi = 1$, is equivalent to the GOS expression for the hydrogen atom in the high energy limit. However, when three terms are kept in Eq. (3), a richer structure emerges

$$F(x^2) = \frac{1}{(1 + x^2)^6} \times \left[R + \frac{r_1}{(1 + \xi_1 x^2)^{n_1}} + \frac{r_2}{(1 + \xi_2 x^2)^{n_2}} \right]. \tag{5}$$

If n_1, n_2, r_1, and r_2, are selected to be real, only a correction to Eq. (4) is introduced. But, if we choose them to be *complex* [and complex conjugate for Eq. (5) to be real], then an entirely new and interesting representation of the GOS emerges which describes it as a *diffraction peak*. This description is well known and has been proposed by De Alfaro and Regge [14]. The n_ℓ are the complex angular momentum Regge poles. This is best understood by expanding Eq. (3) for large K^2 and identifying the result with formula (9.21) of p. 102 of Ref. [14]:

$$F(K^2) \sim \sum_\ell \rho_\ell \xi_\ell^{-n_\ell} (K^2)^{-n_\ell}, \qquad K^2 \text{ large}. \tag{6}$$

Notice that in formula (9.21) of Ref. [14] k is the square root of the impact energy and *not* the momentum transfer, while t is the square of the momentum transfer, and the α's should be identified with the n_ℓ's. The n_ℓ are therefore the complex angular momentum Regge poles; their real part controls the dropoff in the GOS, while the imaginary part is responsible for the oscillatory behavior in the GOS ("hump").

Writing the quantities, yet to be determined, as

$$\xi_1 = \xi_2 = \xi, \qquad n_1 = i\epsilon, \qquad n_2 = -i\epsilon, \qquad r_1 = re^{i\phi}, \quad \text{and} \quad r_2 = re^{-i\phi}, \tag{7}$$

we obtain

$$F(x^2) = \frac{1}{(1 + x^2)^6} \times \left[R + \frac{re^{i\phi}}{(1 + \xi x^2)^{i\epsilon}} + \frac{re^{-i\phi}}{(1 + \xi x^2)^{-i\epsilon}} \right], \tag{8}$$

which can be rewritten as

$$F(x^2) = \frac{1}{(1 + x^2)^6} \{R + 2r \cos[\epsilon \ln(1 + \xi x^2) - \phi]\}. \tag{9}$$

To ensure that $F(x^2)$ is always positive, we impose the restriction that $R \geq 2r$. The limiting case $R = 2r$ corresponds to the vanishing of the GOS in the physical region which occurs only at $E = \infty$ [15].

Clearly Eq. (9) represents a diffraction peak, so that the *hump* is *automatically* embedded in it. Consistent with Eq. (1), we set $\xi = 1$ in Eq. (9) so that our final representation is a four parameter one involving ϵ, R, r, and ϕ

$$F(x^2) = \frac{1}{(1 + x^2)^6} \{R + 2r \cos[\epsilon \ln(1 + x^2) - \phi]\}. \tag{10}$$

To visualize the content of Eq. (10), we *map* Eq. (10) through

$$y = \ln(1 + x^2) \quad \text{and} \quad F^M(y) = (1 + x^2)^6 F(x^2), \tag{11}$$

which reduces Eq. (10) to

$$F^M(y) = a_0 + a_1 \cos\epsilon y + b_1 \sin\epsilon y, \tag{12}$$

where $a_0 = R$, $a_1 = 2r\cos\phi$, and $b_1 = 2r\sin\phi$. Equation (12) represents an expansion of the GOS in *Fourier series* of which we have retained only the first terms, with the OOS being given by

$$\text{OOS} = a_0 + a_1. \tag{13}$$

Clearly, the new representation emphasizes the region of the *hump* rather than the usual [5] small K^2 region. This can be understood theoretically because an analytic function such as defined by Eq. (2) is one block, meaning that its value in any interval defines it everywhere and, in particular, the *hump* defines it completely. From an experimental point of view, the situation is even clearer. Large angle scattering measurements are far more accurate than the small angle ones. Therefore, a greater weight should be given to the former data when producing the final OOS through analytic continuation provided by Eq. (10). In the scaled representation, Eq. (11), we use a weighted square best fit method to obtain the parameters ϵ, R, r, and ϕ, through the functional

$$\mathcal{F} = \sum_{n=1}^{N} \left[\frac{F_n^M - F^M(y_n)}{\Delta F_n^M} \right]^2, \tag{14}$$

where N is the number of experimental data points, y_n, F_n^M, and ΔF_n^M are the mapped *experimental* values through the mapping Eq. (10) of the nth point position, GOS value, and GOS statistical error, respectively. When minimizing $\mathcal{F}$ with respect to a_0, a_1, b_1, and ϵ, we obtain a set of three *linear* equations to determine the first three parameters as a function of the last one, ϵ. Only the last equation which fixes ϵ self-consistently is nonlinear. This is another very pleasant feature of the method.

We illustrate the reliability of this method by applying it to the Xe $P_{1/2}$ and $P_{3/2}$ data at 100 and 500 eV, respectively, where the small angle measurements [5] are still sufficiently accurate [16]. Both our results using only large angle scattering data ($\theta > \theta_c = 4°$ where errors become small) on the one hand, and all the data, on the other hand, are compared with the results obtained using the standard small angle extrapolation formula, Eq. (1). Figure 1 (top part) represents the GOS in the new variables

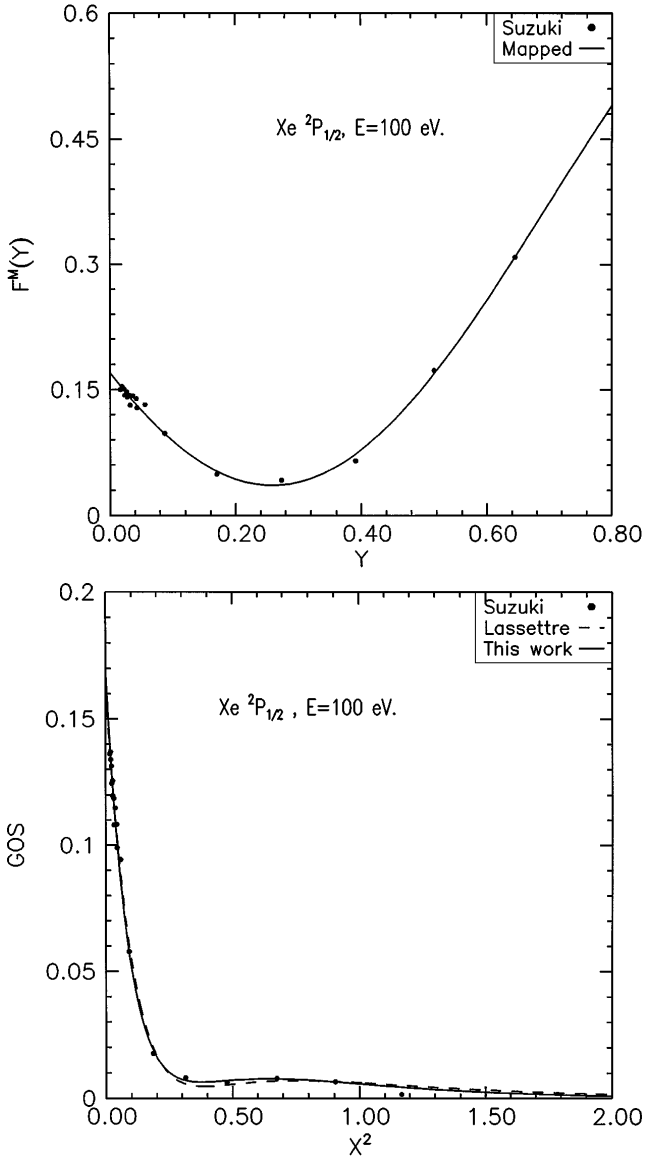

FIG. 1. GOS's for Xe $^2P_{1/2}$ at 100 eV. Top part: experimental data [5], • and our fit, — using mapping Eq. (10). Bottom part: compares the present —, the experimental data [5], • and our fitting of the experimental data [5], – – , using a seven parameter Lassettre expansion to avoid any further unphysical values for the GOS.

given by Eq. (11) for the Xe $P_{1/2}$ at 100 eV. Clearly, the large scattering angle data lead to a reasonably smooth curve but the small angle data form a cluster, and, therefore are unsuitable for analytic continuation.

In Table I we compare our OOS values obtained using all the data points of Suzuki *et al.* [5] for Xe $P_{1/2}$ and Xe $P_{3/2}$ at 100 and 500 eV. Also included are values of OOS's computed with the same data down to only $\theta_c = 4°$. The results are in excellent agreement, within 3%, except for the Xe $P_{1/2}$ state at 500 eV where the reliability [the relative variation between OOS and OOS(4°)] is 18%. This discrepancy is easily understood. From Fig. 2 (top part) we see a strong departure from

TABLE I. Comparison of the OOS for xenon.

Impact	$^2P_{1/2}$		$^2P_{3/2}$	
energy (eV)	100	500	100	500
a_0	0.3638	0.4321	0.1828	0.2943
a_1	−0.1940	−0.2556	0.0320	−0.0785
b_1	0.2645	0.3207	0.1464	0.2622
ϵ	3.6	3.13	7.10	4.50
OOS	0.1698	0.1765	0.2148	0.2158
OOS (4°)	0.1713	0.2114	0.2095	0.2096
Reliability	1.3%	18%	2.5%	3.0%

smoothness in the y representation, therefore making the data inappropriate for analytic continuation. The Xe $P_{3/2}$ OOS at 100 and 500 eV are compatible with the Lassettre limit theorem within 0.5% while for the Xe $P_{1/2}$ the discrepancy is 4%. Table II compares the values of the

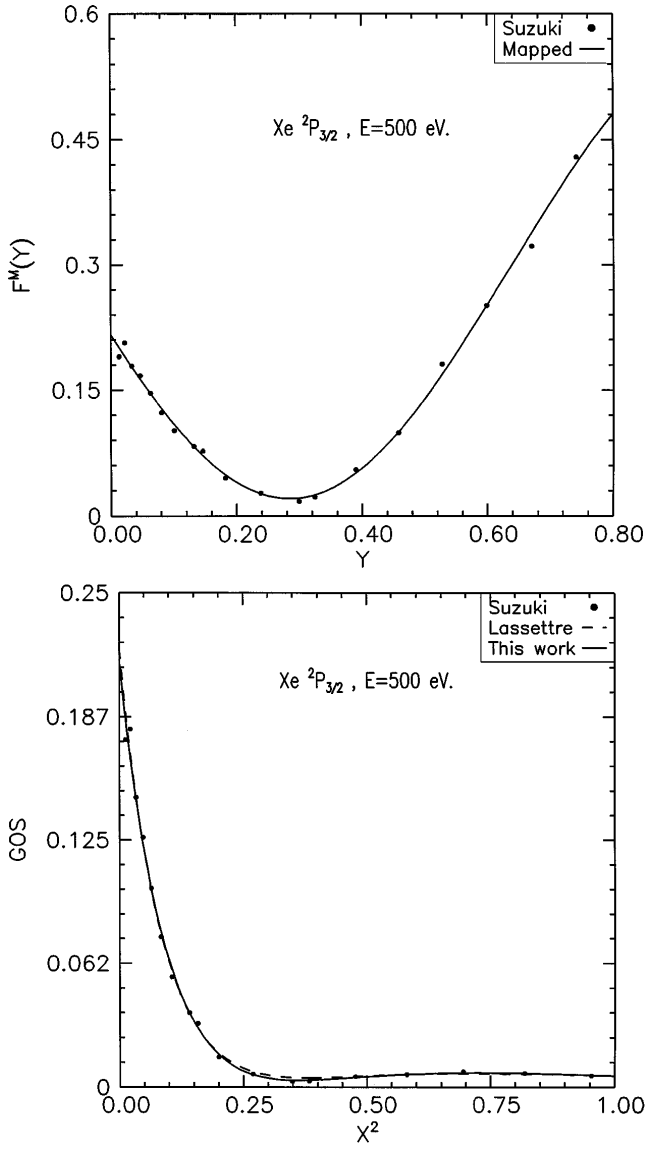

FIG. 2. Same as Fig. 1 but for the case of Xe $^2P_{3/2}$ at 500 eV.

TABLE II. Comparison of the present OOS for xenon with other results.

Author	OOS $^2P_{1/2}$	OOS $^2P_{3/2}$	Ratio $^2P_{3/2}/^2P_{11/2}$
This work	0.173 ± 0.033	0.215 ± 0.001	1.24
D. Bessis *et al.*[a]	(1) 0.141 ± 0.019	0.208 ± 0.027	1.10
	(2) 0.164 ± 0.019	0.223 ± 0.027	1.36
T. Y. Suzuki *et al.*[b]	0.158 ± 0.019	0.222 ± 0.027	1.41
Ester and Kesseler	...	0.23 ± 0.05	...

[a]Reference [13].
[b]Reference [5].
[c]Reference [6].

OOS using all the data points of Suzuki *et al.* [5] for the Xe $P_{3/2}$ and Xe $P_{1/2}$ at 100 and 500 eV with other results. A more complete comparison is found in Ref. [13].

Finally, an experimental procedure to optimize the use of this approach is suggested. (i) The experimental data are remapped in the variables, given by Eq. (11), adjusting the exponent to be $L + M + 5$ as proposed by Klump and Lassettre [9]. (ii) When Fourier analyzing $F^M(y)$, optimization requires that the number of experimental data be a power of 2, 32 would be a good choice, and that the sampling be *uniform in y* (and therefore necessarily not uniform in the scattering angle). Furthermore, a cutoff in the small scattering angles should be made. This can be chosen at the point of increase in the experimental errors. For the present case a cutoff at 4° is a reasonable value. (iii) The Fourier coefficients calculation is accomplished by minimizing the quadratic functional of Eq. (14). A good strategy is to start with the four parameter expansion before going to a higher number of parameters. From the Fourier expansion, the OOS is recovered as $F^M(0) = a_0 + a_1$. For the six parameter case, one would also have to add the a_2 and b_2 terms to the previous expansion. (iv) The violation of the Lassettre theorem provides a good estimate of what could be the final error on the OOS.

We conclude by noting that the present approach exploits the more reliable large scattering angle measurements to obtain more accurate optical oscillator strengths. Because of the fact that this method is model independent and based on first principles dispersion relations, it is applicable to cases involving electron molecule scattering, as well as to cases involving forbidden transitions.

The main interest of the dispersion relation formula Eq. (9), over more traditional fits, is that it allows a *filtering effect* of the experimental fluctuations, because these experimental fluctuations do not satisfy the analytic properties required by the dispersion relation approach. Computer simulated experiments have shown that one order of magnitude can be gained in this filtering process using a formula like Eq. (9), together with a choice of scattering angles defined by our protocol.

This work was supported by the National Science Foundation, DOE, Office of Basic Energy Sciences, Division of Chemical Sciences, and AFOSR. We thank Dr. Z. Chen for valuable discussions.

[1] E. N. Lassettre, A. Skerbele, and M. A. Dillon, J. Chem. Phys. **50**, 1829 (1969).
[2] L. Vuskovic, L. Maleki, and S. Trajmar, J. Phys. B **17**, 2519 (1984).
[3] S. Trajmar, W. Williams, and S. K. Srivastava, J. Phys. B **10**, 3323 (1977).
[4] K. N. Klump and E. N. Lassettre, J. Chem. Phys. **68**, 3511 (1978).
[5] T. Y. Suzuki, Y. Sakai, B. S. Min, T. Takayanagi, K. Wakiya, H. Suzuki, T. Inaba, and H. Takuma, Phys. Rev. A **43**, 5867 (1991), and references therein.
[6] T. Ester and J. Kessler, J. Phys. B **27**, 4295 (1994).
[7] A. Skerbele and E. N. Lassettre, J. Chem. Phys. Lett. **51**, 424 (1978).
[8] K. N. Klump and E. N. Lassettre, J. Chem. Phys. Lett. **51**, 99 (1977).
[9] K. N. Klump and E. N. Lassettre, J. Chem. Phys. **68**, 886 (1978).
[10] E. Gerjuoy and N. Krall, Phys. Rev. **119**, 705 (1960).
[11] M. H. Rubin, R. L. Sugar, and G. Tiktopoulos, Phys. Rev. **162**, 1555 (1967).
[12] A. Tip, in *Invited Papers and Progress Reports of the Tenth International Conference on the Physics of Electronic and Atomic Collisions, Paris, 1977*, edited by G. Watel (North-Holland, Amsterdam, 1977).
[13] D. Bessis, A. Haffad, and A. Z. Msezane, Phys. Rev. A **49**, 3366 (1994).
[14] V. De Alfaro and T. Regge, *Potential Scattering* (North-Holland, Amsterdam, 1965).
[15] Y. K. Kim, M. Inokuti, G. E. Chamberlain, and S. R. Mielczarek, Phys. Rev. Lett. **21**, 1146 (1968).
[16] A. Z. Msezane and Z. Chen, Phys. Rev. A **49**, 3083 (1994).